Danish Meteorological Institute
Ministry for Energy, Utilities and Climate

DMI Report 17-11

A generalised flux Richardson number as a measure of the probability of turbulence generation in upper-tropospheric jet streams

Niels Woetmann Nielsen and Claus Petersen

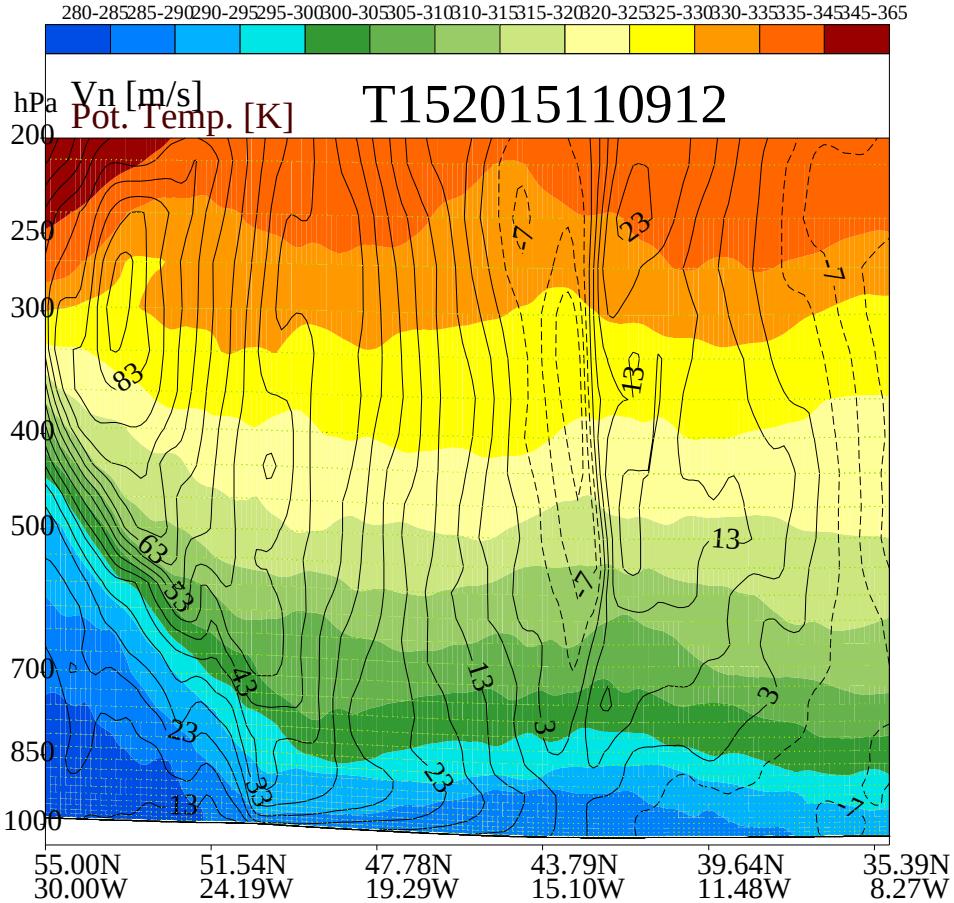

Colophone Serial title:
DMI Report 17-11

Title:
A generalised flux Richardson number as a measure
of the probability of turbulence generation
in upper-tropospheric jet streams

Subtitle:

Authors:
Niels Woetmann Nielsen and Claus Petersen

Other Contributers:

Responsible Institution:
Danish Meteorological Institute

Language:
English

Keywords:
generalised flux Richardson number, horizontal/vertical shear instability, Kelvin-Helmholtz instability, divergence, stretching deformation, shearing deformation, CAT(Clear Air Turbulence) index

Url:
www.dmi.dk/laer-om/dmi-publikationer/2013/17-11

ISSN:
2445-9127

ISBN:
978-87-7478-668-9

Version:
1

Link til hjemmeside:
www.dmi.dk/laer-om/dmi-publikationer/2013

Dansk Resume

Der foreslås et generaliseret flux-Richardson tal,Ri_{f3}, og et dertil hørende generaliseret Richardson tal, Ri_3, som tager hensyn til kompressibilitet og horisontal inhomogenitet i atmosfærens middeltilstand. Ri_{f3} og Ri_3 bliver identisk med de velkendte Richardson tal Ri_f og Ri i det planetare grænselag, hvis dette er stationært, horisontal homogent og med en negligibel middel vertikal vindhastighed. De generaliserede Richardson tal viser at divergens og konvergens, alt andet lige, hhv. reducerer og øger sandsynligheden for generering af turbulens. Shear deformation og produktion af turbulent kinetisk energi via horisontale gradienter af middel vertikal vindhastigheden bridrager til at øge sandsynligheden for generering af turbulens ved at gøre $Ri_{f3} < Ri_f$ og tilsvarende $Ri_3 < Ri$. Det påvises også, alt andet lige, at strækning-deformation kan bidrage til at øge eller mindske sandsynligheden for generering af turbulens, afhængig af både fortegnet paa strækning-deformationen og anisotropien i den horisontale turbulens. I tilfælde af horisontal isotrop turbulens påvirker strækning-deformation ikke sandsynligheden for generering af turbulens. Divergens og strækning-deformation (sidstnæte i tilfælde af anisotrop horisontal turbulens) bidrager til asymmetri i sandsynligheden for generering af turbulens i de bølgende jetstrømme i den øvre troposfære. Nedstrøms for trug og rygge er der hhv. divergens og konvergens, hvilket bidrager til hhv. mindre og større sandsynlighed for generering af turbulens. I jet streaks bidrager divergens i højre indgangsområde og venstre udgangsområde til mindre sandsynlighed for turbulens end i venstre indgangsområde og højre udgangsområde, hvor der er konvergens. Ligeledes er der i jet streaks, alt andet lige, større sandsynlighed for turbulens generering i deres indgangsområde end i deres udgangsområde, hvis den horisontale turbulente kinetiske energi er større på tværs end på langs af jetaksen. Det omvendte gælder, hvis den horisontale turbulente kinetiske energi er størst på langs af jetaksen. Horisontale gradienter i middel potentiel temperatur bidrager til $Ri_{f3} > Ri_f$ og $Ri_3 > Ri$ og gør derfor sandsynligheden for generering af turbulens mindre. Det vises at Ri_{f3} kvalitativt kan forklare de relativt gode resultater, som et meget benyttet "clear air" turbulens indeks giver.

Abstract

A generalised flux Richardson number, Ri_{f3}, and a corresponding generalised gradient Richardson number, Ri_3, are proposed. They take into account horizontal inhomogeneity and compressibility of the mean state. In the steady state, horizontal homogeneous planetary boundary layer with negligible vertical mean wind Ri_{f3} and Ri_3 become identical with the well-known Ri_f and Ri. The generalised Richardson numbers show that anything else equal, divergence reduces and convergence enhances the probability of turbulence generation. Shear deformation and production of turbulent kinetic energy by the horizontal gradient of the mean vertical velocity contribute to an increase in the probability of turbulence generation by making $Ri_{f3} < Ri_f$ and consequently $Ri_3 < Ri$. It is further shown that stretching deformation can contribute to an increase or a decrease in the probability of generation of turbulence, depending on both the sign of the stretching deformation and the anisotropy of the horizontal turbulence. In case of horizontal isotropic turbulence the probability of turbulence generation becomes independent of stretching deformation. Divergence and stretching deformation (the latter in case of anisotropic horizontal turbulence) contribute to an asymmetri in the probability of generation of turbulence in meandering jet streams in the upper troposphere. At jet stream level downstream of troughs there is divergence, contributing to lower probability of turbulence generation, while downstream of ridges there is convergence, contributing to higher probability of turbulence generation. In jet streaks, anything else equal, the probability of turbulence generation is higher in the entrance than in the exit region if the horizontal TKE (turbulent kinetic energy) is larger in the cross-stream than the along-stream direction. The opposite holds if the horizontal TKE is largest in the along-stream direction. It is found that the generalised flux Richardson number qualitatively is able to explain the relative success of a widely used CAT (Clear Air Turbulence) index.

1 Introduction

Three-dimensional (3d) turbulence has been encountered/observed in jet streams both in clear and cloudy air, and in environments with a relative large Richardson number, Ri, typically above the critical value ($Ri_{cr} \approx 0.25$). Characteristic features of upper-tropospheric jet streams are briefly described in Section 2, and Section 3 gives a summary of some mechanisms able to trigger generation of turbulent kinetic energy (TKE). Investigation of cases with clear air turbulence (CAT) has not revealed a strong relationship between CAT and Ri, the latter usually obtained from numerical Weather prediction (NWP) model analyses (e.g. Dotton and Panofsky, 1970; Kaplan et al.,2005). Ri is related to Ri_f, the flux Richardson number. The latter is defined as the ratio of the production of turbulent potential energy (TPE) to the production of TKE in an incompressible, horizontal homogeneous steady state.

The budget equations for TKE, TPE and TTE (the total turbulent energy) are presented in Section 4. The assumptions above are found to describe turbulence in the planetary boundary layer (PBL) reasonably good. It is more questionable how valid these assumptions are in upper-tropospheric jet streams. Here the horizontal gradient of the mean horizontal velocity in certain regions of the jet stream can be of the same order of magnitude as the corresponding vertical gradient. An assumption of horizontal homogeneity does not appear realistic in such regions. This is the motivation for proposing a generalisation of Ri_f, taking into account mean state compressibility and horizontal gradients of mean potential temperature and the full 3d gradient of the 3d mean velocity.

The generalised flux Richardson number, Ri_{f3}, is presented and discussed in Section 5. Ri_{f3} contains both horizontal and vertical turbulent fluxes of momentum and heat. It is found that anisotropy in horizontal turbulence contributes to an asymmetric distribution of probability of turbulence generation in jet streaks. Investigation of severe CAT episodes points to a preference for severe CAT in the entrance region of the jet streak (e.g. Roach, 1970; Reed and Hardy, 1972 and Kaplan et al., 2005). In

Section 5 it is found that due to stretching deformation (D_1) the probability of turbulence, everything else equal, is higher in the entrance region of a jet streak than in its exit region if the horizontal TKE is larger in the cross-stream direction than in the along-stream direction. It is also found that horizontal divergence contributes to higher probability of turbulence generation in the left entrance and right exit region of a jet streak and also to higher probability of turbulence generation downstream of a ridge than downstream of a trough.

It is assumed that the functional relation between Ri_f and Ri proposed by Zilitinkevich et al., 2007, for the horizontal homogeneous, steady state neutral and stable PBL and the inverse relation (Ri as function of Ri_f) also hold in upper-tropospheric jet streams. If it is further assumed that the turbulence is horizontally isotropic D_1 disappears as a parameter in the generalised flux Richardson number.

Section 6 describes how the generalised Richardson number, Ri_3, which for example can be used in place of Ri in a clear air turbulence index, is calculated from Ri_{f3}. The calculation is done in three steps. In the first step Ri_f is calculated from the traditional Ri. In the second step the proposed parameterisation of horizontal turbulent fluxes is used to calculate Ri_{f3}, and in the third step Ri_3 is calculated from Ri_{f3}, using the inverse relation, giving Ri_3 as a function of Ri_{f3}. It is likely that Ri_{f3} can be used directly as the basis for a clear and cloudy air turbulence (CCAT) index and thus avoiding the third step above.

A summary and outlook for future work are given in Section 7.

2 Jet streams

Jet streams are three-dimensional elongated regions of the atmosphere with strong nearly horizontal winds in the core of the jet, surrounded by flow with large vertical and horizontal shear. The horizontal distance across the jet is usually more than 100 times larger than the corresponding vertical distance, and the typical vertical wind shear is usually two orders of magnitude larger than the horizontal shear. A jet stream does not have circular symmetry. The shear is usually largest on the cyclonic shear side of the jet and concentrated in a narrow 'parabolic' shaped frontal zone to the left of the jet core (seen in the flow direction) as well as above and below the jet core. On the anticyclonic shear side of the jet both vertical and horizontal wind shear are usually weaker than on the cyclonic shear side. The thermal stratification (static stability) tends to be largest on the cyclonic shear side within the frontal zones and smaller on the anticyclonic shear side. The shear zones are regions with a potential for triggering three-dimensional turbulence. Figure (1) shows a typical example of a vertical cross-section approximately perpendicular to the jet stream, showing potential temperature and the horizontal wind speed normal to the plane.

3 Shear instability

3.1 Horizontal and vertical shear instability

The method used to investigate if a given basic state of the atmosphere may become unstable to small perturbations is called linear stability analysis. Such analyses have shown that a necessary but insufficient condition for instability in a basic state without thermal stratification is presence of local extremes of the basic state relative vorticity (e.g. Markowski and Richardson, 2010) defined by $\overline{\vec{\zeta}} = \overline{\zeta}_x \cdot \vec{i} + \overline{\zeta}_y \cdot \vec{j} + \overline{\zeta}_z \cdot \vec{k}$, where $\overline{\zeta}_x = \frac{\partial \overline{w}}{\partial y} - \frac{\partial \overline{v}}{\partial z}$ and $\overline{\zeta}_y = \frac{\partial \overline{u}}{\partial z} - \frac{\partial \overline{w}}{\partial x}$ are the horizontal components and $\overline{\zeta}_z = \frac{\partial \overline{v}}{\partial x} - \frac{\partial \overline{u}}{\partial y}$ the vertical component of the basic state relative vorticity vector. Note here that we consider only so small spatial scales of the basic state that the planetary vorticity, f, can be treated as

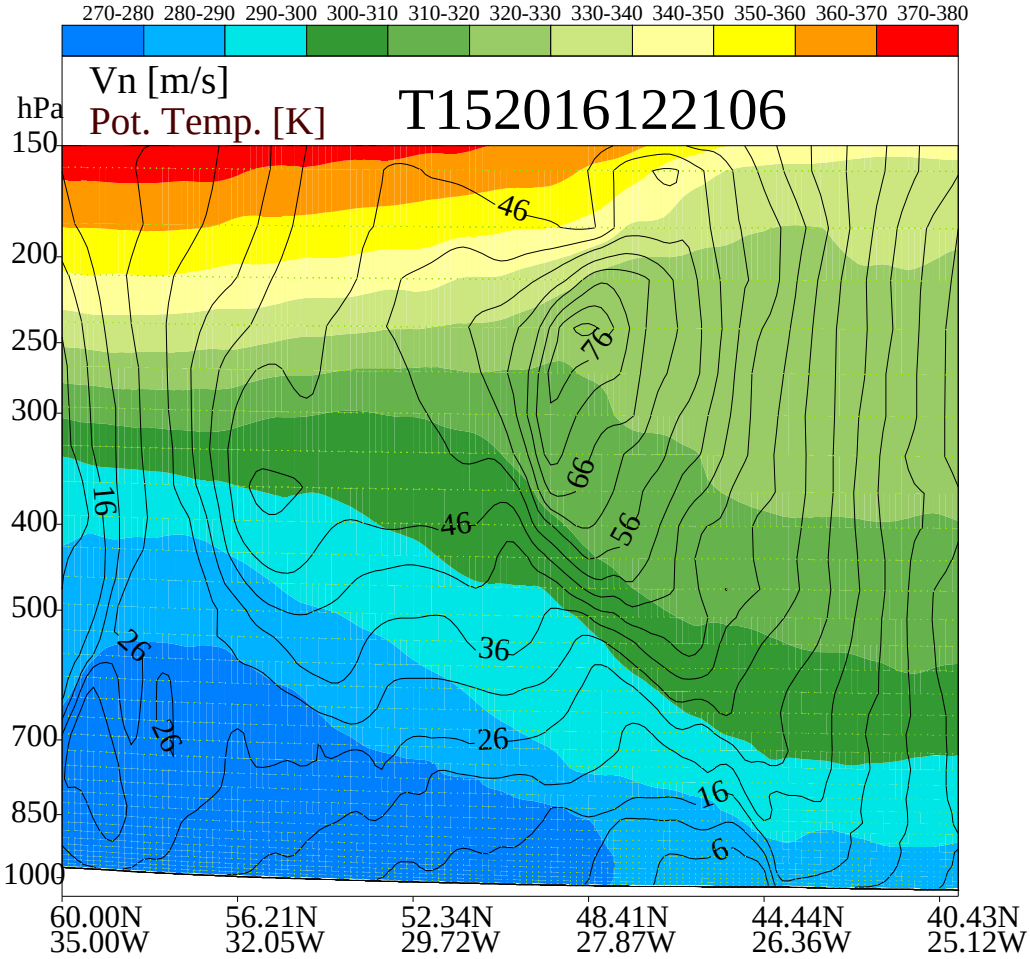

Figure 1: Vertical cross section approximately normal to the jet stream, showing potential temperature in coloured 10 K intervals and horizontal wind speed normal to the plane in 5 m/s intervals.

a constant, which means that we are not discussing barotropic instability.

3.2 Kelvin-Helmholtz instability

If the basic state is stably stratified the vertical shear instability is replaced by Kelvin-Helmholtz (KH) instability, stating that a necessary, but insufficient condition for instability is that $Ri < 0.25$, where $Ri = N^2/S_z^2$ with $N^2 = \beta\frac{\partial\overline{\theta}}{\partial z}$, $\beta = \frac{g}{\overline{\theta}}$ and $S_z^2 = \left(\frac{\partial\overline{\vec{V}_h}}{\partial z}\right)^2$. $\overline{\vec{V}_h}$ is the basic state horizontal wind velocity, $\overline{\theta}$ the basic state potential temperature and g is gravity.

4 Turbulent energy budgets

Total turbulent energy is the sum of turbulent kinetic energy (TKE) and turbulent potential energy (TPE). The budget equation for TKE, with the assumption of incompressibility of the fluctuating part of the flow ($\nabla \cdot \vec{V'} = 0$), is

$$\frac{DE_K}{Dt} + \nabla \cdot \vec{\phi'} = -\tau_{ij}\frac{\partial\overline{u_i}}{\partial x_j} + \beta F_{\theta z} - \epsilon_K, \tag{1}$$

where $E_K = \frac{1}{2}(\overline{u'^2} + \overline{v'^2} + \overline{w'^2})$ is the turbulent kinetic energy, $\vec{\phi'} = \frac{1}{\rho_0}\overline{p'\vec{V'}} + \frac{1}{2}\overline{e\vec{V'}}$, $e = u'^2 + v'^2 + v'^2$, $F_{\theta z} = \overline{w'\theta'}$ and ϵ_K the dissipation of TKE. The first term on the right side of (1) is the shear production term for TKE, written in tensor notation (for each $i = 1, 2, 3$ with j running from 1 to 3). The budget

for TPE is

$$\frac{DE_P}{Dt} + \nabla \cdot \vec{\phi'}_P = -\left(\frac{\beta}{N}\right)^2 \left(F_{\theta x}\frac{\partial \overline{\theta}}{\partial x} + F_{\theta y}\frac{\partial \overline{\theta}}{\partial y}\right) - \beta F_{\theta z} - \epsilon_P, \tag{2}$$

where $E_P = \left(\frac{\beta}{N}\right)^2 E_\theta$, $E_\theta = \frac{1}{2}\overline{\theta'^2}$, $\vec{\phi'}_P = \left(\frac{\beta}{N}\right)^2 \vec{\phi'_\theta}$, $\vec{\phi'}_\theta = \frac{1}{2}\overline{\theta'^2 \vec{V}'}$ and $\epsilon_P = \left(\frac{\beta}{N}\right)^2 \epsilon_\theta$, where ϵ_θ is the dissipation of potential temperature fluctuations. In (2) $F_{\theta x} = \overline{u'\theta'}$ and $F_{\theta y} = \overline{v'\theta'}$ are the horizontal turbulent heat fluxes. In the derivation of (2) it is assumed that N changes slowly compared to turbulent variations (Zilitinkevich et al., 2007).

The budget equation for total turbulent energy (TTE) is obtained by adding (1) and (2), giving

$$\frac{DE}{DT} + \nabla \cdot \vec{\phi_T} = -\tau_{ij}\frac{\partial \overline{u_i}}{\partial x_j} - \left(\frac{\beta}{N}\right)^2 \left(F_{\theta x}\frac{\partial \overline{\theta}}{\partial x} + F_{\theta y}\frac{\partial \overline{\theta}}{\partial y}\right) - \epsilon_T, \tag{3}$$

where $\nabla \cdot \vec{\phi_T} = \nabla \cdot \vec{\phi_K} + \nabla \cdot \vec{\phi_P}$ and $\epsilon_T = \epsilon_K + \epsilon_P$. The term $\beta F_{\theta z}$, which is the buoyancy production term in the TKE equation, does not appear in (3) since it appears in (1) and (2) with opposite signs. According to (3) the only production terms for TTE are the shear production of TKE and production of TPE due to horizontal turbulent heat fluxes, the latter given by

$$H_f = -\left(\frac{\beta}{N}\right)^2 \left(F_{\theta x}\frac{\partial \overline{\theta}}{\partial x} + F_{\theta y}\frac{\partial \overline{\theta}}{\partial y}\right). \tag{4}$$

For our purpose it is convenient to write the shear production in the form

$$S_3 = S_u + S_v + S_w \tag{5}$$

with

$S_u = -\overline{u'u'}\frac{\partial \overline{u}}{\partial x} - \overline{u'v'}\frac{\partial \overline{u}}{\partial y} - \overline{u'w'}\frac{\partial \overline{u}}{\partial z}$, $S_v = -\overline{v'u'}\frac{\partial \overline{v}}{\partial x} - \overline{v'v'}\frac{\partial \overline{v}}{\partial y} - \overline{v'w'}\frac{\partial \overline{v}}{\partial z}$

and

$S_w = -\overline{w'u'}\frac{\partial \overline{w}}{\partial x} - \overline{w'v'}\frac{\partial \overline{w}}{\partial y} - \overline{w'w'}\frac{\partial \overline{w}}{\partial z}$.

S_3 can be written as

$$S_3 = \Pi - \frac{1}{2}\delta\left(\overline{u'u'} + \overline{v'v'}\right) - \overline{w'w'}\frac{\partial \overline{w}}{\partial z} - \frac{1}{2}D_1\left(\overline{u'u'} - \overline{v'v'}\right) - D_2\overline{u'v'} - \overline{w'u'}\frac{\partial \overline{w}}{\partial x} - \overline{w'v'}\frac{\partial \overline{w}}{\partial y}. \tag{6}$$

Here $\Pi = -\overline{u'w'}\frac{\partial \overline{u}}{\partial z} - \overline{v'w'}\frac{\partial \overline{v}}{\partial z}$ is the turbulent production of TKE due to vertical shear of the horizontal wind in the basic flow, $\delta = \frac{\partial \overline{u}}{\partial x} + \frac{\partial \overline{v}}{\partial y}$ is the horizontal divergence and $D_1 = \frac{\partial \overline{u}}{\partial x} - \frac{\partial \overline{v}}{\partial y}$ and $D_2 = \frac{\partial \overline{v}}{\partial x} + \frac{\partial \overline{u}}{\partial y}$ are the stretching and shearing deformation, respectively.

5 A generalised flux Richardson number

In a horizontal homogeneous stably stratified basic (mean) state of the planetary boundary layer (PBL) $H_f = 0$ and $S = \Pi$. In this PBL the only production term for TPE is $-\beta F_{\theta z}$ and in the TKE equation the only production term is $S = \Pi$. A flux Richardson number,Ri_f, is defined as the ratio of the production of TPE to the production of TKE, i.e. $Ri_f = \frac{-\beta F_{\theta z}}{\Pi}$. We define a generalised flux

Richardson number, Ri_{f3}, which is also applicable in atmospheric jet streams with basic (mean) states that can be horisontal inhomogeneous and compressible. Ri_{f3} is based on (2) and (6) and becomes

$$Ri_{f3} = Ri_f \frac{1 + R_{tpe}}{1 + R_{tke}} \tag{7}$$

with

$$R_{tpe} = \left(\frac{\beta}{N}\right)^2 \frac{F_{\theta x}\frac{\partial \overline{\theta}}{\partial x} + F_{\theta y}\frac{\partial \overline{\theta}}{\partial y}}{\beta F_{\theta z}} \tag{8}$$

and

$$R_{tke} = R_{div} + R_{def} + R_{wsh} \tag{9}$$

In (9)

$$R_{div} = -\frac{\frac{1}{2}\delta\left(\overline{u'^2} + \overline{v'^2}\right) + \overline{w'^2}\frac{\partial \overline{w}}{\partial z}}{\Pi}, \tag{10}$$

$$R_{def} = R_{def1} + R_{def2} \tag{11}$$

and

$$R_{wsh} = -\frac{\overline{w'u'}\frac{\partial \overline{w}}{\partial x} + \overline{w'v'}\frac{\partial \overline{w}}{\partial y}}{\Pi} \tag{12}$$

In (11)

$$R_{def1} = -\frac{1}{2}\frac{D_1(\overline{u'^2} - \overline{v'^2})}{\Pi} \tag{13}$$

and

$$R_{def2} = -\frac{D_2\overline{u'v'}}{\Pi}. \tag{14}$$

Due to on average down-gradient turbulent transports of heat, R_{tpe} is non-negative and therefore only can contribute to $Ri_{f3} \geq Ri_f$. In the same way (due to on average down-gradient turbulent transports of momentum) R_{def2} in (11) and R_{wsh} in (12) are non-negative and therefore contribute to $Ri_{f3} \leq Ri_f$.

However, R_{div} in (10) can be positive or negative, depending on the signs of δ and $\frac{\partial \overline{w}}{\partial z}$. The same holds for R_{def1} in case of anisotropic horizontal turbulence ($\overline{u'^2} \neq \overline{v'^2}$).

5.1 Asymmetric probability of turbulence generation due to divergence

According to (10) horizontal divergence ($\delta > 0$) and vertical divergence ($\frac{\partial \overline{w}}{\partial z} > 0$) both contribute to $Ri_{f3} \geq Ri_f$, whereas horizontal convergence ($\delta < 0$) and vertical convergence ($\frac{\partial \overline{w}}{\partial z} < 0$) contribute to $Ri_{f3} \leq Ri_f$. The probability of turbulence generation, anything else equal, is therefore largest/smallest in regions with horizontal and vertical convergence/divergence. In upper-tropospheric jet streams areas with horizontal convergence are typically found between ridge and downstream trough (e.g. Palmén and Newton, 1969) and in the left entrance and right exit regions of jet streaks (Uccellini and Kocin, 1987). An example of an idealised linear jet streak is shown in Figure 2. In the upper troposphere the numerical value of horizontal divergence tends to be at a maximum close to the tropopause. Since the atmosphere is only weakly compressible

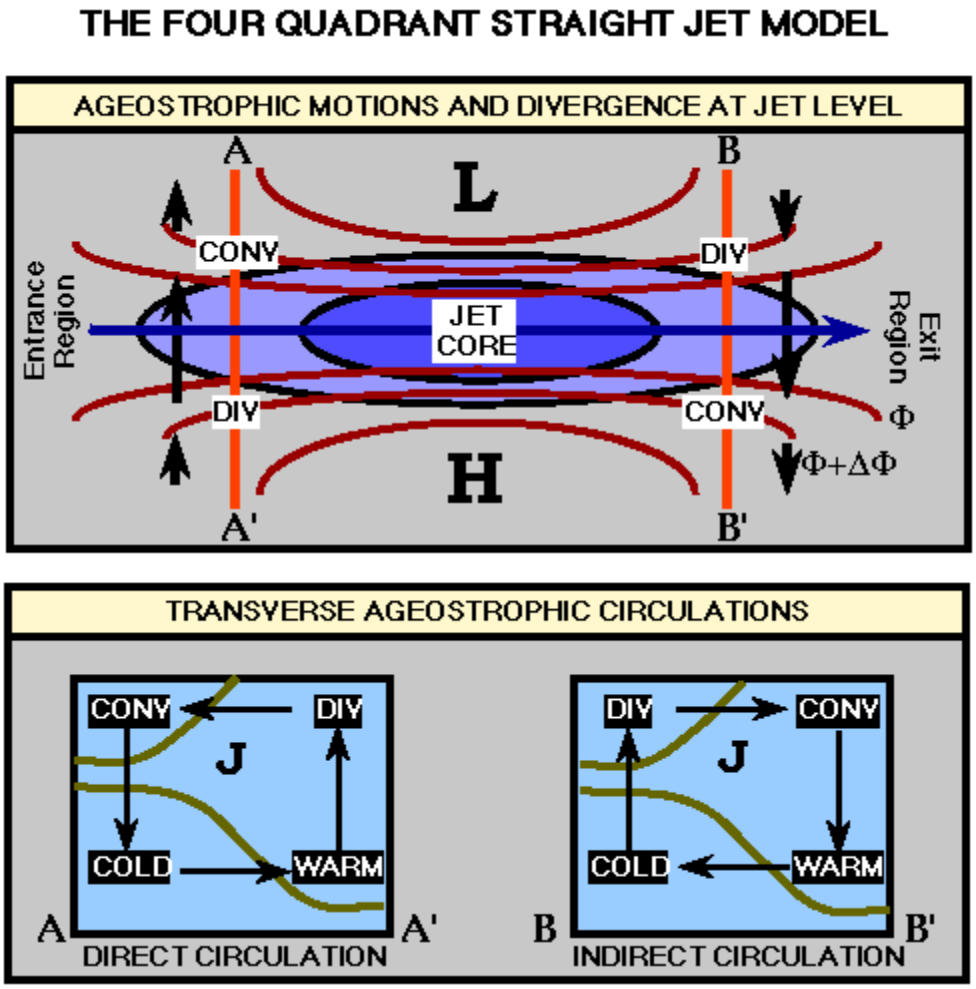

Figure 2: Idealised picture of a linear jet streak. Top figure is a horizontal plane view, showing isotacs (black contours) and geopotential height (dark-red contours). Black arrows show the ageostrophic wind, and the jet streak induced ageostrophic circulations in vertical planes perpendicular to the jet axis are shown in the bottom figure in the entrance and exit region of the jet streak. (From www4.ncsu.edu, a variant of a figure in Kocin and Uccellini, 1990).

(implying opposite signs of δ and $\frac{\partial \overline{w}}{\partial z}$ in regions with large $|\delta|$) the two terms in (10) have opposite signs, and it may not universally hold that δ and R_{div} have opposite signs. This is investigated more closely by rewriting (10) in the form

$$R_{div} = \frac{\delta E_K \left(-1 + 3A_z\right)) - 2A_z \cdot E_K \nabla \cdot \overrightarrow{V}}{\Pi}. \tag{15}$$

Here $A_z = \frac{E_{Kz}}{E_K}$ and $E_{Kz} = \frac{1}{2}\overline{w'^2}$. If the mean state is incompressible ($\nabla \cdot \overrightarrow{V} = 0$) and the turbulence is isotropic ($A_z = 1/3$) it follows from (15) that $R_{div} = 0$. If the turbulence is isotropic and the atmosphere is compressible, R_{div} has opposite sign of $\nabla \cdot \overrightarrow{V}$, and if the atmosphere is incompressible and the turbulence is anisotropic with $A_z < 1/3$, R_{div} has opposite sign of δ. The actual atmosphere is nearly incompressible (δ and $\frac{\partial \overline{w}}{\partial z}$ are of nearly the same magnitude, but with opposite signs) and its turbulence is anisotropic. Zilitinkevich et al., 2007 estimated $A_z \approx 0.25$ in the neutral PBL with a decrease with increasing Ri asymptotically to $A_z \approx 0.075$ at very large Ri. Similar anisotropy is expected in upper-tropospheric jet streams. For these reasons R_{div} and δ are expected to have opposite signs in regions with relatively large $|\delta|$, with enhanced and reduced probability of turbulence in regions with large convergence and divergence, respectively. In summary for jet streaks it is found that

anisotropic turbulence due to divergence contributes to an asymmetric distribution of the probability of turbulence generation. Anisotropy with $A_z < \frac{1}{3}$ enhances the probability of turbulence in the left entrance and right exit region and diminishes this probability in the right entrance and left exit region.

5.2 Asymmetric probability of turbulence generation due to horizontal deformation

In case of anisotropic horizontal turbulence, it is noted that R_{def1} contributes to an asymmetric distribution of the probability of turbulence generation in jet streaks. This can for example be seen by rewriting R_{def1} as

$$R_{def1} = -\frac{D_1(\gamma - 1)(1 - A_z)}{(\gamma + 1)\Pi}. \tag{16}$$

Here $\gamma = \frac{A_x}{A_y}$, $A_x = \frac{E_{Kx}}{E_K}$, $A_y = \frac{E_{Ky}}{E_K}$, $E_{Kx} = \frac{1}{2}\overline{u'^2}$ and $E_{Ky} = \frac{1}{2}\overline{v'^2}$. If $\gamma < 1 (A_x < A_y, E_{Kx} < E_{Ky})$ it follows from (16) that $R_{def1} > 0$ if $D_1 > 0$ and $R_{def1} < 0$ if $D_1 < 0$. In the entrance/exit region of a zonal jet streak (along-stream direction from west to east) $D_1 > 0 / D_1 < 0$. Therefore, everything else equal, Ri_{f3} is smaller in the entrance than in the exit region and consequently, the probability of turbulence generation is highest in the entrance region, while the opposite is the case if $\gamma > 1 (E_{Kx} > E_{Ky})$, i.e. if the horizontal along-stream TKE is larger than the cross-stream TKE.

In a coordinate system with the x-axis rotated an angle α from direction west to east to the downstream direction of the horizontal flow in the jet stream R_{def1} can be written

$$R_{def1} = -\frac{D_{1r}(\overline{u_r'^2} - \overline{v_r'^2})}{2\Pi}, \tag{17}$$

where subscript r refers to the rotated system. In the latter system $D_{1r} = D_1 \cos 2\alpha + 2 \cdot D_2 \sin\alpha \cos\alpha$ and $D_{2r} = D_2 \cos 2\alpha - 2 \cdot D_1 \sin\alpha \cos\alpha$, implying that the resultant deformation $D = ({D_1}^2 + {D_2}^2)^{1/2}$ is invariant to a rotation of the coordinate system. In case of horizontal anisotrophy ($\gamma \neq 1$), R_{def1} can be written

$$R_{def1} = \frac{(D_1 \cos 2\alpha + 2D_2 \sin\alpha \cos\alpha) \cdot \overline{v_r'^2}(1 - \gamma)}{2\Pi} \tag{18}$$

(18) behaves qualitatively in agreement with the theoretical expectation. For illustration a meridional jet streak with north as the down-stream direction is considered. In this case $\alpha = \frac{\pi}{2}$, giving $D_{1r} = -D_1$ and $R_{def1} = -\frac{D_1}{\Pi}\frac{1}{2}\overline{v'^2}(1 - \gamma)$. In the entrance and exit region $D_1 < 0$ and $D_1 > 0$, respectively, implying $R_{def1} > 0$ in the entrance region and $R_{def1} < 0$ in the exit region. Accordingly, the probability of turbulence generation due to stretching deformation is highest in the entrance region. This result is valid for horizontal anisotropic turbulence with largest TKE in the cross-stream direction of the jet streak ($\gamma < 1$). The opposite result is obtained if TKE is largest in the along-stream direction ($\gamma > 1$).

6 Calculation of a generalised Richardson number

The NWP model calculates Ri (valid for a horizontal homogeneous mean state). Next Ri_f is calculated from

$$Ri_f = \frac{1.25Ri(1 + 36Ri)^{1.7}}{(1 + 19Ri)^{2.7}}, \tag{19}$$

a function of Ri proposed by Zilitenkevich et al., 2007. Ri_{f3} is then calculated from (7) (in practice a parameterised version of this equation). In the next step it is assumed that the relation between Ri_{f3}

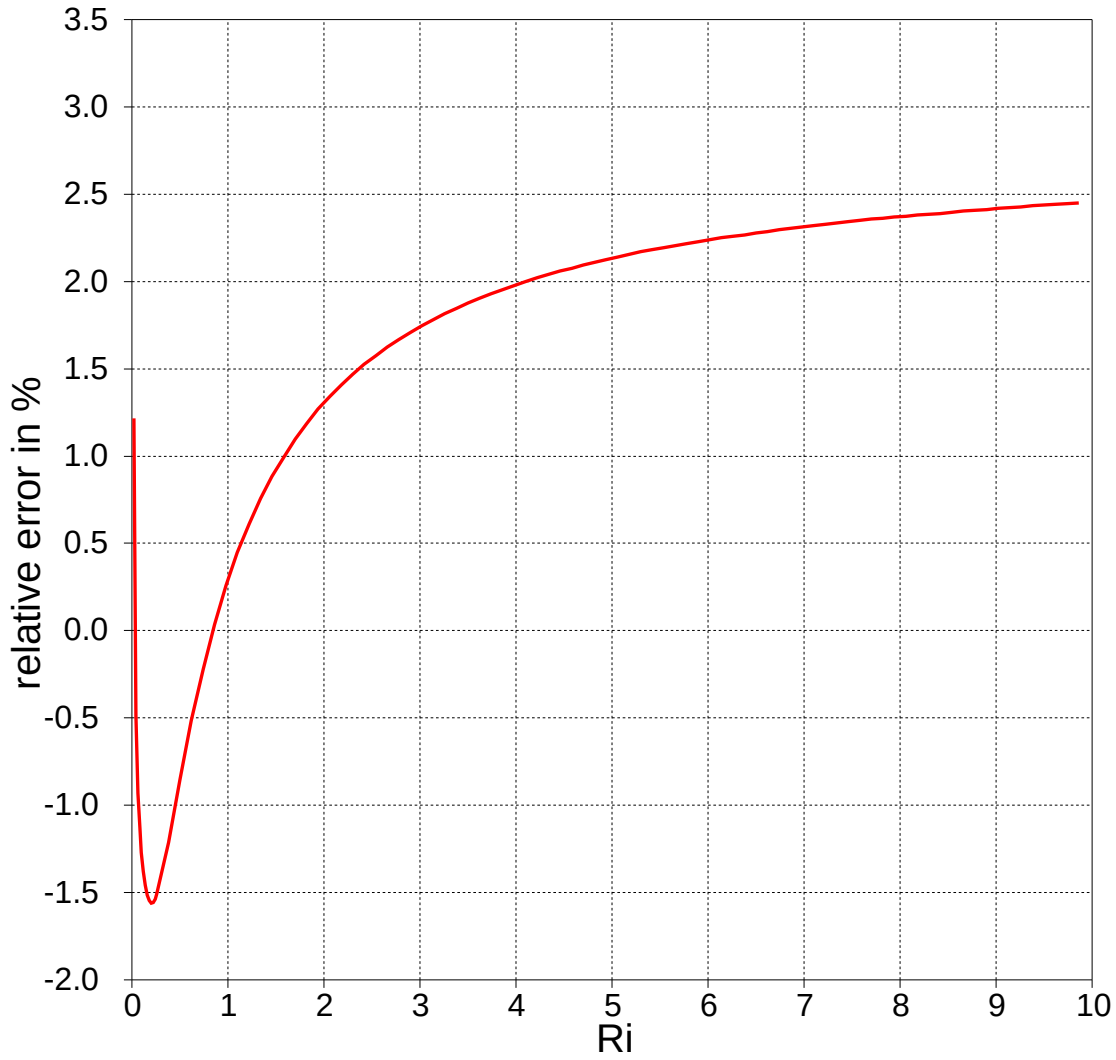

Figure 3: Relative error in Ri obtained by first calculating Ri_f from (19) and then using Ri_f to recalculate Ri from (20)

and Ri_3 is the same as for Ri_f and Ri. A reverse relationship between Ri and Ri_f can be written approximately

$$Ri \approx 0.8Ri_f \frac{1-3.61Ri_f}{1-\left(\frac{Ri_f}{Ri_{f\infty}}\right)^{1-2.56*Ri_f}} - 0.08 \cdot Ri_f - Ri_f^2, \tag{20}$$

and with the assumption given above we also have

$$Ri_3 \approx 0.8Ri_{f3} \frac{1-3.61Ri_{f3}}{1-\left(\frac{Ri_{f3}}{Ri_{f3\infty}}\right)^{1-2.56\cdot Ri_{f3}}} - 0.08 \cdot Ri_{f3} - Ri_{f3}^2, \tag{21}$$

with $Ri_{f3\infty} = Ri_{f\infty} = 1.25\frac{36^{1.7}}{19^{2.7}} \approx 0.2$. Here $Ri_{f\infty}$ is the asymptotic value of Ri_f for $Ri \to \infty$. As the last step Ri is replaced by Ri_3. The latter is calculated from (21). Finally, Ri_{f3} is not allowed to become larger than $Ri_{f\infty}$ by using the constraint $Ri_{f3} = min\,(Ri_{f3}, Ri_{f\infty})$. According to Figure (3) the relative error of Ri in percent calculated by the procedure above varies from about -1.6% to about 2.5% in the Ri-range from 0.02 to 10 and does not exceed 2.8% out to $Ri = 120$ (figure not shown). The calculation of Ri_f from Ri followed by calculation of Ri_{f3} from (7) and finally calculation of

Ri_3 from (21) is considered accurate enough for practical use, for example in a clear and cloudy air (CCAT)-index. In a follow-up report it will be investigated if a CCAT index can be based solely on Ri_{f3} and thus avoiding the third step in the above calculations.

7 Summary and outlook

In the present report we propose a generalised flux Richardson number, Ri_{f3}, that takes into account horizontal inhomogeneity that can become significant in certain regions of the atmosphere, not least in upper-tropospheric meandering jet streams. Ri_{f3} introduces an asymmetry in the probability of generation of turbulence in meandering jet streams. First of all the asymmetry is due to divergence, contributing to higher probability of turbulence generation downstream of ridges than downstream of troughs and in jet streaks to higher probability of turbulence generation in their left entrance and right exit regions than in their right entrance and left exit regions (Figure (2)).

If the turbulence is horizontally anisotropic in jet streaks an asymmetry is also created by horizontal stretching deformation. In case of largest horizontal TKE in the cross-jet streak direction the horizontal stretching deformation will contribute to higher probability of turbulence generation in the entrance than in the exit of a jet streak. The opposite will be the case if the along-stream TKE is largest.

To the authors knowledge it is unknown to what extend - if at all - the turbulence in upper-tropospheric jet streams is horizontally anisotropic. A discussion of the impact of anisotropy is given here, but due to the uncertainties about horizontal anisotropy the stretching deformation term will not be taken into account in a follow-up report, investigating if Ri_{f3} or Ri_3 can be used successfully in a clear and cloudy air (CCAT) index. Since the numerical weather prediction model applied in the latter investigation does not calculate horizontal turbulent transport terms it is necessary to parameterise these terms. How this is done will be described in the follow-up report.

Finally, we briefly discuss the qualitative behaviour of Ri_{f3} and a widely used clear air turbulence (CAT) index. The latter index, defined by $I_{cat} = |\overrightarrow{\frac{V_h}{\partial z}}|(D - \delta)$, is derived from the frontogenetic intensity function (Petterssen, 1956). In I_{cat}, $D = (D_1^2 + D_2^2)^{1/2}$ is the resultant deformation. Larger values of I_{cat} means larger probability of turbulence generation. It can be seen that the probability of turbulence generation in both I_{cat} and Ri_{f3} increases with larger vertical wind shear, larger resultant deformation and larger convergence. However, unlike Ri_{f3}, I_{cat} does not contain separate information about D_1 and D_2, and also lacks any information about static stability of the air. The former implies that I_{cat} is unable to take into account effects of possible anisotropic horizontal turbulence in jet streaks, which introduces an asymmetry in the probability of generation of turbulence in the entrance (frontogenetic) and exit (frontolysis) region of the jet streak. The latter means that I_{cat} remains unchanged regardless of the static stability of the air, although the expectation is that the probability of turbulence generation decreases with increasing static stability. Despite these differences between I_{cat} and Ri_{f3}, the latter seems theoretically to explain the reported relative success of I_{cat}.

References

[J. A. Dutton, and H. A. Panofsky] Clear Air Turbulence: A mystery may be unfolding. Science, 167, 937-944.

[G. P. Ellrod and D. J. Knapp 1992] An objective clear-air turbulence forecasting technique: Verification and operational use. Wea. Forecasting, 7, 150-165.

[M. L. Kaplan, A. W. Huffman, K. M. Lux, J. J. Charney, A. J. Riordan, and Y.-L. Lin] Characterizing the Severe Turbulence Environments Associated with Commercial Aviation Accidents. Part 1: A 44 Case Study Synoptic Observational Analyses. Meteorrol. Atmos. Phys., 88, 129-152.

[P. J. Kocin, and L. W. Uccellini 1990] Snowstorms Along the Northeastern Coast of the United States: 1955 to 1985. Meteor. Monogr., 22, No. 44, 280 pp.

[P. Markowski, and Y. Richardson 2010] Mesoscale Meteorology in Midlatitudes. Wiley-Blackwell

[N. W. Nielsen, and C. Petersen 2012] An upper-tropospheric clear and cloudy air turbulence index in DMI-HIRLAM. DMI-scientific report 12-01. www.dmi.dk/laer-om/generelt/dmi-publikationer/videnskabelige-rapporter.

[E. Palmén, and C. W. Newton 1969] Atmospheric Circulation systems: Their Structure and physical Interpretation. Academic Press, International geophysics series, Vo. 13, Ch. 6.1, 140-144.

[S. Petterssen 1956] Weather Analysis and Forecasting. Vol. 1. McGraw-Hill Book Co., 428 pp.

[L. W. Uccellini, and P. J. Kocin 1987] The interaction of jet streak circulations during heavy snow events along the east coast of the United States. Wea. Forecasting,1,289-308.

[R. J. Reed, and K. R. Hardy,1972] A case study of persistent, intense clear air turbulence in an upper-level frontal zone. J. Appl. Meteor., 12, 541-549.

[W. T. Roach, 1970] On the influence of synoptic development on the influence of high level turbulence. Quart. J. Roy. Meteor. Soc., 96, 413-429.

[S. S. Zilitinkevich, T. Elperin, N.Kleeorin, and I. Rogachecskii, 2007] Energy- and flux-budgets (EFB) turbulent closure model for stably stratified flows. Part 1: steady state, homogeneous regimes. Atmospheric Boundary Layers. Nature, Theory, and Applications to Environmental Modelling and Security (A. Baklanov, B. Grisogono, Eds.). Springer, 11-35.